ELSEVIER

Journal of Chromatography A, 760 (1997) 89–103

JOURNAL OF CHROMATOGRAPHY A

Combination of the steric mass action and non-ideal surface solution models for overload protein ion-exchange chromatography

Poonam Raje, Neville G. Pinto*

Department of Chemical Engineering, University of Cincinnati, Cincinnati, OH 45221-0171, USA

Abstract

A model has been developed for protein ion-exchange equilibria under overloaded chromatographic conditions. This model combines the steric mass action model with the non-ideal surface solution model and accounts for steric hindrance and nearest neighbor interactions between protein–protein, protein–salt and salt–salt in a single formalism. Using the model on protein ion-exchange data, the importance of obtaining ion-exchange heat measurements in addition to adsorption isotherms has been demonstrated. It has been shown that small inaccuracies in the heat of ion-exchange data can lead to large differences in predictions of elution behavior. Additionally, it has also been shown that salt–salt interactions on the surface can strongly influence protein adsorption and that in the presence of these interactions, the shape and orientation of the molecule on the surface are important.

Keywords: Adsorption isotherms; Steric mass action model; Non-ideal surface solution model; Heat of adsorption; Proteins

1. Introduction

The stringent requirement of purity standards in pharmaceutical, food and other biotechnology industries related to human consumption has focused attention on bioseparation and purification techniques. As the commercialization of biotechnology progresses, the need to develop cost effective downstream processing techniques is becoming more intense. Chromatographic purification steps, normally the most expensive steps, are thus prime targets for reducing costs.

High-performance ion-exchange chromatography (HPIEC) is widely employed for the purification of biomolecules [1]. It is important for the economics of the process that the chromatographic separation be overloaded. In contrast to analytical operations, in which a linear equililbrium description is adequate, the non-linear isotherm region is invariably important for overloaded chromatography. The lack of an appropriate model to adequately describe non-linear equilibria has significantly impeded the design and optimization of preparative chromatography.

Traditionally, the characterization of competitive non-linear adsorption employs multicomponent Langmuir isotherms. However, this formalism provides an unsatisfactory description of equilibrium adsorption behavior [2,3] and, furthermore, is thermodynamically inconsistent [4,5]. Consequently, significant efforts are being made to develop thermodynamically consistent models for protein adsorption.

The stoichiometric displacement model (SDM) of Kopaciewicz et al. [6] and Rounds and Regnier [7] was originally proposed to describe protein retention in linear ion-exchange chromatography and later was applied to overloaded protein chromatography [8,9]. This approach models the process of ion-exchange as

*Corresponding author

PII S0021-9673(96)00812-6

a stoichiometric reaction described by the mass-action principle. It assumes that ion exchange is the only mechanism for adsorption, the entire ion-exchange capacity is available to the protein for adsorption and that the surface and mobile phases are thermodynamically ideal.

The steric mass action model (SMA) proposed by Brooks and Cramer in 1992 [10] uses the framework of SDM and explicitly accounts for the steric hindrance of salt counterions upon protein binding in multicomponent equilibria. The concentration of hindered salt ions is related to the protein surface concentration through the steric factor σ which is assumed to be constant for each protein. The concept is intuitively appealing and the model has been shown to have some predictive capability.

The non-ideal surface solution (NISS) model proposed by Li and Pinto in 1994 [11] is a thermodynamically consistent equilibrium model that is also based on the SDM. The adsorbed phase is modeled as a non-ideal surface solution in equilibrium with a non-ideal bulk liquid. Non-idealities are characterized by surface and liquid activity coefficients. In the liquid phase, the major source of non-ideal behavior is assumed to be interactions between modulator ions while non-ideal surface behavior is assumed to be dominated by nearest neighbor interactions between adsorbed proteins.

It is desirable to develop a model that is completely general for protein ion-exchange equilibrium. In order to achieve this, it is necessary to account for all important specific and non-specific adsorption effects in a thermodynamically consistent manner. These include ion exchange, steric effects, Van der Waals and electrostatic interactions between adsorbed proteins and salts, and hydrophobic interactions between proteins and the adsorbate. While a complete thermodynamic description of each of these effects is desirable, it is difficult. Also, the intricacy of such an inclusive model would limit its applicability. It is therefore important to identify the major factors that influence protein ion exchange, to enable reliable engineering design and optimization of chromatographic separations.

In this article, we present a theoretical framework that includes both steric effects and nearest neighbor lateral interactions, by combining the SMA and the NISS models. Using this framework, the importance of including both these non-ideal effects is demonstrated. Both SMA and NISS have been used separately in the past to describe selected overload protein chromatography data. However, both of these models differ in their basic tenet with regard to the effect that limits protein adsorption. It will be shown, through an analysis with the combined model, why these models have worked in the past. Furthermore, it will also be shown that adsorption isotherm data are not sufficient to unambiguously interpret the significance of the coefficients in each of the models when used separately.

2. Theoretical development

2.1. SMA–NISS model

As has already been stated, the model takes the basic theoretical framework of the NISS model given by Li and Pinto [11] and incorporates the steric factor defined by Brooks and Cramer [10].

The formalism employs the following assumptions:

- Competitive binding in ion-exchange systems can be represented by mass-action equilibrium, where electroneutrality on the stationary phase is maintained;
- The effect of the co-ion can be neglected in the ion-exchange process [9,12];
- The multipointed nature of protein binding can be represented by an experimentally determined characteristic charge [9] and
- Non-ideal effects such as aggregation, change in the tertiary structure of the protein and hydrophobic interactions with the stationary phase are negligible.

The adsorption of $n-1$ macromolecules 1, 2,...$n-1$ is considered in the presence of a small counterion (salt) n, called the modulator. Due to the adsorption of the macromolecules, some of the adsorbed salt counterions may be sterically hindered and hence unavailable for stoichiometric exchange with proteins in solution. The equilibrium description of the system is given by:

$$c_1 + \frac{z_1}{z_n}\bar{n}_n \Leftrightarrow n_1 + \frac{z_1}{z_n}c_n$$

$$c_2 + \frac{z_2}{z_n}\bar{n}_n \Leftrightarrow n_2 + \frac{z_2}{z_n}c_n$$

.....

.....

$$c_{n-1} + \frac{z_{n-1}}{z_n}\bar{n}_n \Leftrightarrow n_{n-1} + \frac{z_{n-1}}{z_n}c_n \quad (1)$$

where c_i and n_i are the bulk and surface concentrations of i, respectively, and $\bar{n}_n$ is the surface concentration of salt ions available for ion exchange.

The concentration of hindered salt ions is proportional to the surface concentration of $n-1$ macromolecules through the steric factor σ [10]:

$$\hat{n}_n = \sum_{i=1}^{i=n-1} \sigma_i n_i$$

$$n_n = \bar{n}_n + \hat{n}_n \quad (2)$$

where $\hat{n}_n$ is the surface concentration of hindered salt ions and n_n is the total surface concentration of salt ions.

For ion-exchange reactions, the equilibrium constants are related to the species activities (a_i) by:

$$K_{ni} = \frac{a_i^s}{a_i}\left(\frac{a_n}{a_n^s}\right)^{z_i/z_n} \qquad i = 1\ldots n-1 \quad (3)$$

In the adsorbed phase,

$$a_i^s = \frac{\gamma_i^s x_i z_i}{z_r} \qquad i = 1\ldots n-1$$

$$\overline{a_n^s} = \frac{\gamma_n^s \overline{x_n} z_n}{z_r} \quad (4)$$

where x_i is the surface mol fraction, z_i is the charge number and γ_i^s is the surface activity coefficient of species i and z_r is the charge number of the resin.

In the mobile phase,

$$a_i = c_i \qquad i = 1\ldots n-1$$

$$a_n = \gamma_n c_n \quad (5)$$

Eq. (4) assumes that the standard state for the adsorbed species corresponds to that of complete saturation of the ion-exchange capacity by the species. The maximum surface concentration possible for any species i is λ/z_i mmol/kg resin. In this state, there is no other competing species on the surface, making it an ideal state (surface activity coefficient is unity). In Eq. (5) it is assumed that the solution activity coefficients of proteins is one, since the molar concentration of proteins is generally small. The standard state for the mobile phase salt is assumed to be the hypothetical state, if the solute obeyed Henry's law all the way to 1 m*M*.

Substituting Eqs. (4) and (5) in Eq. (3),

$$K_{ni} = \frac{\gamma_i^s z_i x_i}{z_r c_i}\left(\frac{\gamma_n c_n z_r}{\gamma_n^s z_n \overline{x_n}}\right)^{z_i/z_n} \qquad i = 1\ldots n-1 \quad (6)$$

Also, by definition, the total ion-exchange capacity of the adsorbent is:

$$\lambda = \sum_{i=1}^{n-1}(\sigma_i z_n + z_i)n_i + z_n\overline{n_n}$$

Thus, it follows that:

$$z_r = \sum_{i=1}^{n-1}(\sigma_i z_n + z_i)x_i + z_n\overline{x_n} \quad (7)$$

since λ/z_r is the molar ion-exchange capacity of the resin and $x_i = n_i/(\lambda/z_r)$ is the surface mole fraction of the adsorbed component.

Eqs. (6) and (7), in conjunction with appropriate equations for the activity coefficients in the surface phase and for the modulator in the liquid phase, constitute the equilibrium model.

2.1.1. Surface activity coefficients

As before [11], Talu and Zweibel's [14] equation is employed for the calculation of the activity coefficients in the surface phase

$$\ln(\gamma_i^s) = -S_i \ln\left(\sum_{j=1}^{n}\omega_j\alpha_{ji}\right) + S_i - S_i\sum_{j=1}^{n}\frac{\omega_j\alpha_{ij}}{\sum_{k=1}^{n}\omega_k\alpha_{kj}} \qquad i = 1\ldots n \quad (8)$$

where S_i is the adsorbate shape factor and ω_i is the surface fraction defined as:

$$\omega_j = \frac{S_j x_j}{\sum_{k=1}^{n} S_k x_k} \tag{9}$$

α_{ij} is the Boltzmann weighting factor for local compositions. It is calculated using Wilson's method [15,19] for incorporating differences in intermolecular forces between components of the adsorbed phase. α_{ij} is related to the average lateral interaction energy between segments of nearest-neighbor molecules by:

$$\alpha_{ij} = \exp\left[-\frac{C}{2kT}(e_{ij} - e_{jj}) \right] \tag{10}$$

where C is the coordination number for the adsorbed segments. The energy of interaction parameters e_{ij} and e_{jj} are functions of the spreading pressure. Talu and Zweibel [14] showed that at low temperatures, e_{jj} can be calculated from pure component isosteric heat of adsorption data:

$$e_{jj} = \frac{q_{j\pi} - q_{j0}}{\frac{C}{2}NS_j} \tag{11}$$

where $q_{j\pi}$ is the isosteric heat of adsorption of pure j at the same spreading pressure as the mixture, and q_{j0} is the isosteric heat of adsorption at zero spreading pressure. The cross-energy parameters are calculated from:

$$e_{ij} = (e_{ii}e_{jj})^{1/2}(1 - \beta_{ij}) \tag{12}$$

where β_{ij} is an empirical factor that accounts for differences in size and adsorptive properties of the molecules.

2.1.2. Modulator activity coefficients

The method developed by Bromley [16] has been found to be effective for modeling the activity of strong electrolytes up to an ionic strength of about 6 M. In terms of the ionic strength (I), of the liquid, the Bromley equation is expressed as:

$$\ln(\gamma_n) = \frac{-0.511\sqrt{I}|z_+z_-|}{1+\sqrt{I}} + \frac{(0.06+0.6B)|z_+z_-|I}{\left(1+\frac{1.5}{|z_+z_-|}I\right)^2} + BI \tag{13}$$

This equation contains a single coefficient, B, which is readily available for all salts commonly used as modulators in protein ion-exchange chromatography.

2.2. Column model

The equilibrium model was combined with a kinetic model for a column packed with a porous adsorbent to provide a mathematical description of the chromatographic process. For a species i, the column equations are:

$$\frac{\delta c_i}{\delta \tau} = -\frac{\delta c_i}{\delta X} + \frac{1}{Pe_i}\frac{\delta^2 c_i}{\delta X^2} - \phi St_i(n_i^* - n_i)$$

$$\frac{\delta n_i}{\delta \tau} = St_i(n_i^* - n_i) \tag{14}$$

where Pe and St are the Peclet and Stanton numbers, respectively, τ and X are the dimensionless time and distance, and n_i^* is the surface concentration at equilibrium with c_i. For the isocratic elution mode, the following conditions apply:

Initial conditions

For $0 \le x \le L$

$$c_i = n_i = 0 \qquad i = 1\ldots n-1$$

$$c_n = c_{nF}$$

$$\overline{n_n} = \frac{\lambda}{z_n}$$

Boundary conditions

At $X = 0$

For $0 \le \tau \le \tau_{\text{feed}}$

$$c_i = c_{iF} + \frac{1}{Pe}\frac{\delta c_i}{\delta X} \qquad i = 1\ldots n$$

For $\tau \ge \tau_{\text{feed}}$

$$c_i = \frac{1}{Pe}\frac{\delta c_i}{\delta X} \qquad i = 1\ldots n-1$$

$$c_n = c_{nF} + \frac{1}{Pe}\frac{\delta c_n}{\delta X}$$

Table 1
Protein ion-exchange equilibrium isotherms

Protein	Ion exchanger	Modulator	Ref.
BSA	Matrex silica PAE-1000 (Amicon) weak anion exchanger diameter, 10 μm average pore size, 1000 Å	NaCl-207 m*M*	[17]
α-chymotrypsin	SCX-sulfopropyl (Waters) strong cation exchanger diameter, 8 μm	Na_3PO_4-75 m*M*	[10]
Cytochrome *c*	SCX-sulfopropyl (Waters) strong cation exchanger diameter, 8 μm	Na_3PO_4-75 m*M*	[10]

At $X = 1$

$$\frac{\delta c_i}{\delta X} = 0 \qquad i = 1 \ldots n$$

3. Results and discussion

3.1. Characterization of adsorption isotherms

The combined SMA–NISS model was applied to three protein adsorption isotherms reported in the literature [17,10]. The conditions for each isotherm measurement are summarized in Table 1. Application of the SMA–NISS model in each case involves the estimation of seven parameters, summarized in Table 2. Also shown in Table 2 are the methods used to evaluate each of these parameters. Most of these methods have been recommended in the original development for each of the models [10,11]. Some parameters have been estimated differently in this work for reasons that will be discussed.

Both the SMA and NISS models estimate the SDM coefficients z_i and K_{ni} from linear isocratic elution data. It can be shown that under linear conditions:

$$\ln(k') = \ln(K_{n1}\phi) - \frac{z_1}{z_n}\ln(\gamma_n c_n) \qquad (15)$$

It should be noted that Eq. (15) contains an activity coefficient correction for the liquid phase (γ_n). Li and Pinto [17] have shown that it is important to incorporate this correction in evaluating SDM coefficients. In particular, they have shown that the value of the equilibrium constant is strongly affected by the activity of the solution, while the effective charge is relatively insensitive to it. This can be explained on the basis of Fig. 1, where the mobile phase activity coefficient of the two salts used in the selected protein isotherm data are plotted as a

Table 2
Method of evaluation of SMA–NISS parameters

Parameter	Origin of coefficient	Method of evaluation
Characteristic charge of protein z_i	SDM	Linear isocratic elution
Equilibrium constant K_{ni}	SDM	Linear isocratic elution
Shape factor of protein S_i	NISS	Molecular dimension in solution
Steric factor of protein σ_i	SMA	Error Plot
Change in the isosteric heat of adsorption for protein $q_{in} - q_{i0}$	NISS	Calorimetric measurement
Change in the isosteric heat of adsorptiion for salt $q_{n\pi} - q_{n0}$	NISS	Calorimetric measurement
Cross interaction parameter, β	NISS	Multicomponent data

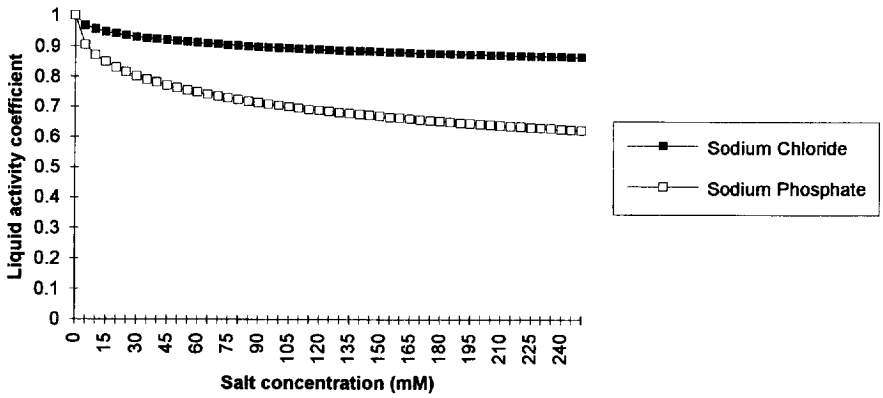

Fig. 1. Effect of salt concentration on the liquid activity coefficients.

function of mobile phase concentration (c_n) using Eq. (13). From the graph it can be seen that for the range of salt concentrations in which linear isocratic elution is carried out, γ_n, though significantly different from 1, does not change very much with concentration. The implication of this (Eq. (15)) is that the slope, z_i, is essentially unaffected by the introduction of γ_n, while the intercept changes significantly, affecting the value of the equilibrium constant K_{ni}.

Using Eq. (13) for estimating activity coefficients of single salt electrolytes, z_i and K_{ni} values in Table 3 were calculated from experimental data reported in the literature [10].

Table 3
Equilibrium coefficients for the SMA–NISS model

	BSA	α-Chymotrypsin	Cytochrome *c*
z_1	4.9107	4.8	6
K_{n1}	$2.175 \cdot 10^{10}$	$3.99 \cdot 10^{8}$	$7.98 \cdot 10^{11}$
S_1	13.55	6.35	4.745
S_n	1	1	1
B	0.0574	0.0043	0.0043
λ	360 mequiv./kg resin	567 m*M*	567 m*M*
z_r	1	1	1
z_+, z_-	1,1	1,3	1,3

The shape factor, S_i, originates from the NISS model and is defined as the ratio of the free perimeter of the protein molecule to that of a standard molecule [18]. Here the modulator is considered as the standard molecule. The shape factor quantifies the total number of external, lateral contacts of the protein. Previously [17], it was calculated based on the assumption that on saturation, proteins completely occupy the adsorbent surface area available. This assumption does not hold when we consider steric hindrance of salt ions, as steric hindrance implies that there is some fraction of ion-exchange sites that are not available to the protein for ion exchange. In this study, molecular dimensions of the protein and the modulator in solution have been used to estimate the shape factor and are reported in Table 4. It should be noted that this approach inherently assumes that the shape of the molecule is not significantly changed by ion exchange. Previous research has indicated that some proteins change conformation on adsorption. Also, it is possible that proteins reorient themselves in

Table 4
Molecular dimensions of species in solution

Species	Shape	Dimensions	Shape factor	Ref.
BSA	Ellipsoid	140×40×40 Å	13.55	[21]
α-Chymotrypsin	Ellipsoid	51×40×40 Å	6.35	[22]
Cytochrome *c*	Spherical	34 Å	4.745	[22]
Chloride ion	Spherical	3.32 Å	1	[20]
Sodium ion	Spherical	3.58 Å	1	[20]

overloaded conditions in order to minimize the free energy. In the light of such possible conformation and orientation changes, the calculation of shape factor using molecular dimensions in solution is open to question. A more correct estimation of shape factor would require data on the conformation of a protein after adsorption and also on the orientation of the protein as a function of surface concentration. Though such a description is desirable, present methods of imaging adsorbed proteins make this difficult to measure. It is, therefore, useful to study the sensitivity of adsorption behavior to the shape factor. With this objective, as a first approximation, the shape factor was calculated from the species' molecular dimensions in solution. In the event that the model is found to have high sensitivity to the shape factor, a more sophisticated method of evaluation will have to be used.

All surface interactions, other than the primary ion-exchange interaction, are quantified in the NISS model through the isosteric heat of adsorption. A rigorous evaluation of this involves calorimetric measurements that cover the composition space of interest with respect to both the modulator and protein. In order to circumvent these measurements, Li and Pinto [11,17] assumed the following: (a) Isosteric heat can be estimated from the temperature dependence of adsorption isotherms through a Clausius-Clapeyron type equation; (b) within a limited protein concentration range, the variation of the isosteric heat is linear with surface coverage according to the equation

$$q_{1\pi} - q_{10} = mz_1x_1 \tag{16}$$

where m will change with the modulator concentration; and (c) lateral interactions between adsorbed salt ions is negligible; i.e.,

$$q_{n\pi} - q_{n0} = 0 \tag{17}$$

With these assumptions, the only unknown coefficient in the model is m (Eq. (16)), and its value was obtained from best fits of adsorption isotherm data.

In contrast to this approach, in the SMA model all non-ideal effects, i.e., effects other than those considered by SDM, are assumed to be negligible, except for steric hindrance. This effect is quantified through the steric factor, which is obtained as a fit parameter from isotherm data.

It is clear from this discussion that the SMA and NISS models each neglect different non-ideal effects that may have a significant influence on protein ion exchange. Also, since both models ultimately rely on ion-exchange isotherm fits, this implies that the effect not considered, although important, may have been lumped into the fit parameter, which could then be misinterpreted.

The combined SMA–NISS model offers an opportunity to gauge the relative importance of each of the non-ideal effects. With this objective, adsorption equilibrium isotherms were generated for each of the protein ion-exchange systems listed in Table 1. As mentioned earlier, a simulation of the combined SMA–NISS model requires the seven parameters listed in Table 2. For these simulations, parameters z_1 and K_{n1} were obtained from the reported values in the references listed in Table 1. The shape factors were calculated from the reported molecular dimensions in liquid, as shown in Table 4. As in Li and Pinto's work [11,17], it was assumed that salt–salt lateral interactions on the surface ($q_{n\pi} - q_{n0}$) were negligible, thus obviating the need to estimate the cross interaction parameter β. The parameters used for simulation and their values are listed in Table 3.

The adsorption equilibrium isotherms were generated using the parameter values in Table 3 using a standard numerical subroutine [13], for a range of m (Eq. (16)) and σ values in order to find the best fit values for each protein system reported in Table 1. At each m and σ value, the cumulative error between the simulated and experimental isotherms was calculated from:

$$\text{Error} = \sqrt{\sum_{i=1}^{\text{data-points}} (n_i^{\text{model}} - n_i^{\text{experimental}})^2} \tag{18}$$

A typical plot for the variation of error in the $\sigma - m$ space is shown in Fig. 2; this particular plot is for BSA ion exchange. Two important features are immediately evident. First, the very large error associated with the $m=0$, $\sigma=0$ case implies that SDM by itself provides a very poor description of protein ion exchange, and it is essential to correct for non-ideal effects. Secondly, there are a range of m and σ values that define the minimum error trough, and this trough extends from the $\sigma=0$ face to the $m=0$ face. To illustrate this, three sets of $m-\sigma$

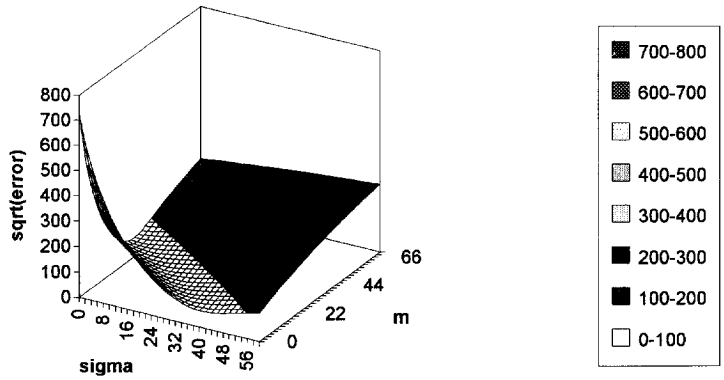

Fig. 2. Cumulative error curve as a function of model coefficients for BSA.

combinations from the minimum error set were used to simulate adsorption isotherms for each protein; these are shown in Figs. 3–5. It is seen that in all cases the three sets provide equally good fits of the data. Also shown in these figures are the corresponding SDM isotherms. As expected, SDM greatly overpredicts the experimental data.

Column simulations with the minimum error combinations of σ and m give expected results. Shown in Fig. 6 are overload elution simulations for BSA at two sample volumes, 20 and 500 μl. These simulations were performed with the parameters shown in Table 5. At 20 μl (Fig. 6a), the system is in the linear region of the isotherm and all four simulations, the three $\sigma-m$ minimum combinations and the SDM overlap. Under linear conditions, non-ideal effects such as surface interactions and steric hindrance are not important since surface coverage is low. At the higher loading of 500 μl (Fig. 6b), which corresponds to non-linear equilibrium, there is a significant difference between the SDM prediction and the SMA–NISS predictions. Furthermore, it should be noted that all three $\sigma-m$ minimum error combinations give essentially the same elution profile.

The observation that the minimum error trough extends from the $\sigma=0$ to the $m=0$ face in Fig. 2 explains why the NISS and SMA models can separately characterize isotherm data effectively (Figs. 3–5), even though they account for completely different non-ideal effects. Also, since other combinations of σ and m can provide equally good fits, the fit parameters obtained from the SMA and NISS models are lumped parameters whose physical significance is difficult to interpret. Furthermore, and very importantly, these results show that adsorption

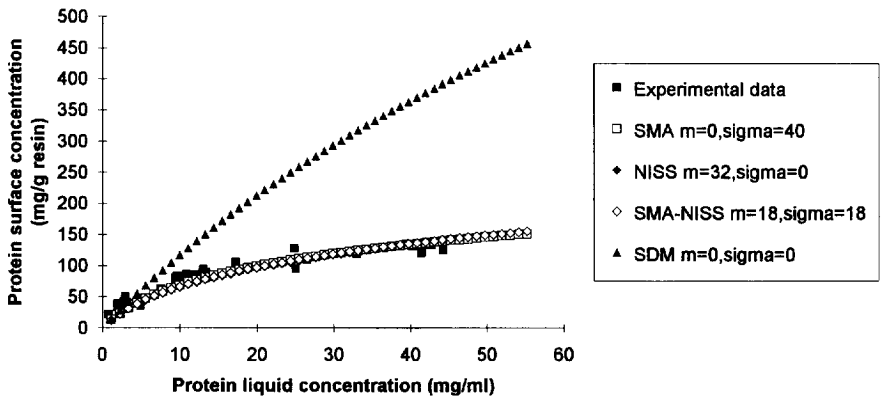

Fig. 3. Adsorption isotherm fits for BSA.

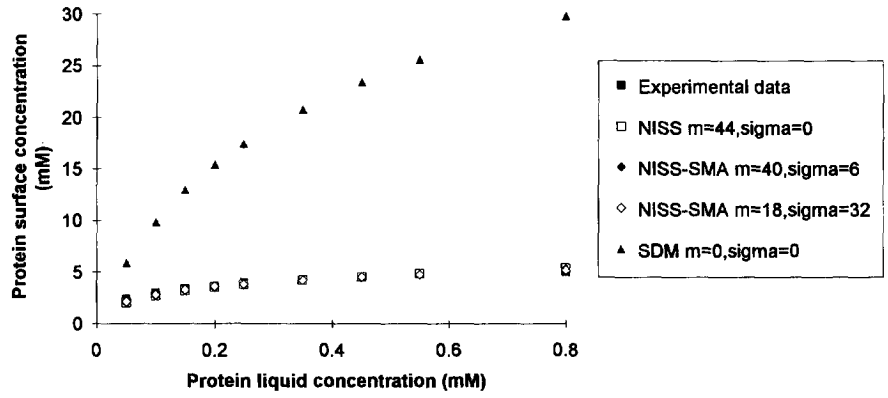

Fig. 4. Adsorption isotherm fits for α-chymotrypsin.

isotherm data alone are insufficient to obtain insight into the relative importance of the steric hindrance and surface interactions.

Talu and Zweibel's UNIQUAC model [18] for adsorbed phases suggests that surface non-idealities due to nearest neighbor interactions can be quantified by measurements of the isosteric heat of adsorption. Thus, if calorimetric measurements are combined with isotherm measurements it should be possible to separately evaluate the surface interaction contribution with the SMA–NISS framework. Since calorimetric measurements are generally difficult to make, it is useful to evaluate the sensitivity of the SMA–NISS predictions to the accuracy of the calorimetric data. If the model is relatively insensitive to the heat data, the assumption made by Li and Pinto [11] earlier, i.e., the estimation of isosteric heat from a Clausius-Clapeyron type equation, may be valid; the advantage of this assumption is that calorimetric measurements are not necessary, since the effect can be estimated from isotherm data at a sufficient number of temperatures. It should, however, be noted that such an approach lumps any changes in the conformation of the protein due to the temperature change along with the lateral interactions.

3.2. Sensitivity to protein heat of adsorption

The sensitivity of the SMA–NISS model to the heat of ion-exchange data is illustrated for the BSA case using the adsorption isotherm corresponding to $m=18$ $\sigma=18$. For this particular protein, the isosteric heat of adsorption varies with surface concentration as follows:

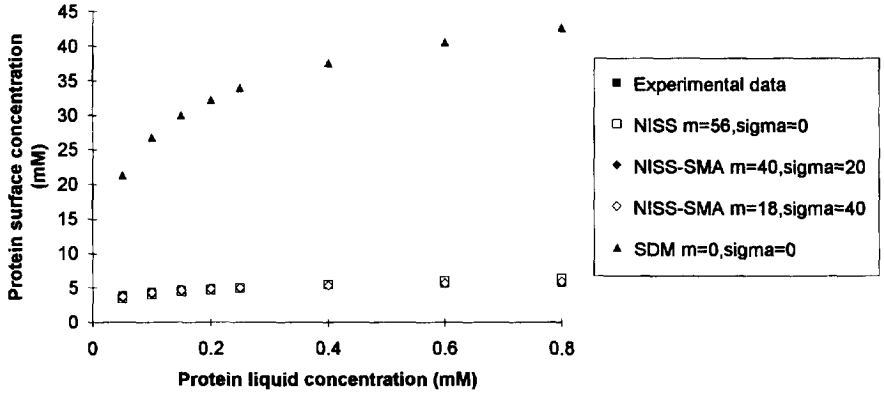

Fig. 5. Adsorption isotherm fits for cytochrome *c*.

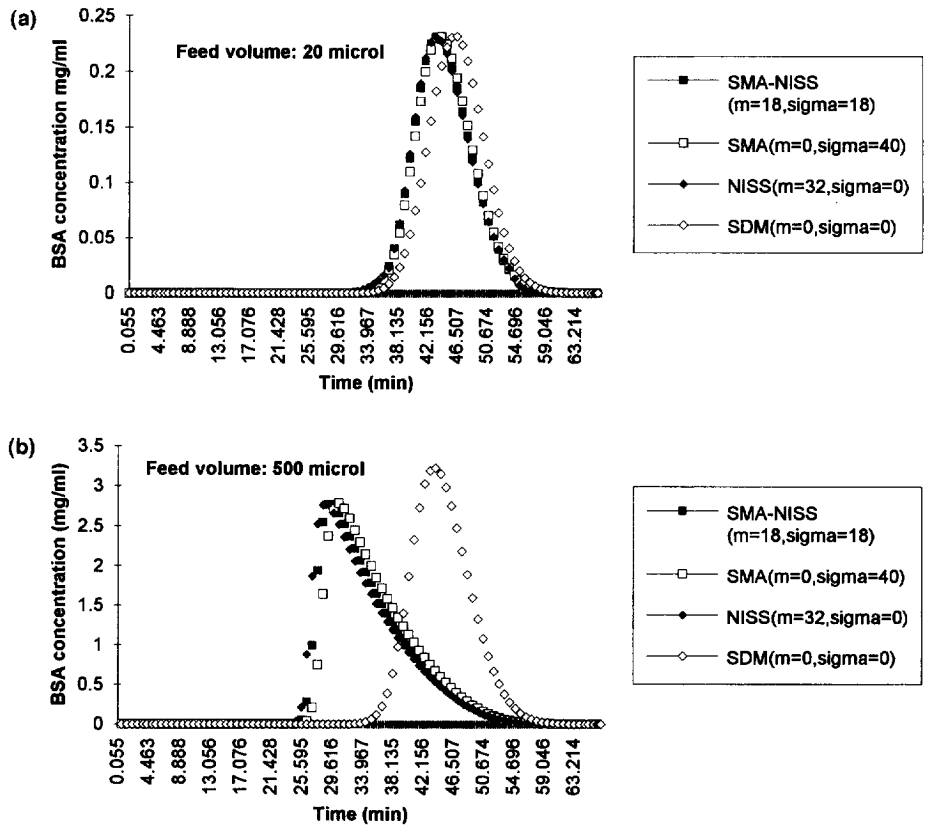

Fig. 6. (a) Simulation of isocratic elution of BSA with a feed volume of 20 μl. (b) Simulation of isocratic elution of BSA with a feed volume of 500 μl.

$$q_{1\pi} - q_{10} = mz_1x_1 \tag{19}$$

Since the isosteric heat of adsorption is defined as:

$$q_{1\pi} = \frac{\delta Q}{\delta\left(\frac{\lambda \cdot 10^{-3}x_1}{z_r}\right)} \tag{20}$$

Table 5
Simulation parameters for isocratic elution simulations of BSA

Length	25 cm
Diameter	0.46 cm
Flow-rate	1 ml/min
Dead time	3.3 min
c_{1F}	0.889 m*M*
c_n	207 m*M*
Distance step dX	0.0025
Time step $d\tau$	0.00558
St_1, St_n	20, 30
Pe	10^6

this implies that the corresponding heat of adsorption (from integration of Eq. (20) after substitution of Eq. (19)) is:

$$Q = a(z_1x_1)^2 + b(z_1x_1)$$

$$\text{where } a = \frac{m\lambda \cdot 10^{-3}}{2z_rz_1} \text{ and } b = \frac{q_{10}\lambda \cdot 10^{-3}}{z_rz_1} \tag{21}$$

To examine the sensitivity to heat of adsorption, a different functional form of heat of adsorption was selected:

$$Q = \frac{a(z_1x_1)}{b + (z_1x_1)} \tag{22}$$

Assigning a and b values of 0.005 and 0.035, respectively, gives the heat of adsorption curve shown in Fig. 7. It can be seen that Eqs. (21) and (22) give very similar values of Q, and the maximum

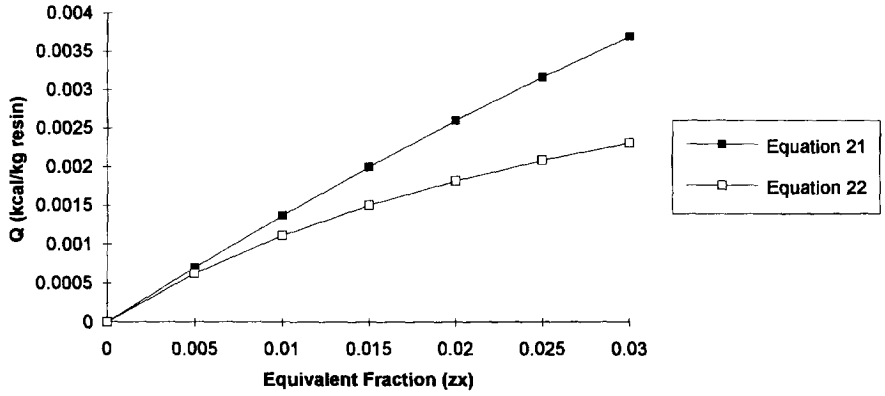

Fig. 7. Selected variations of heat of adsorption with concentration.

difference between the two curves is, approximately, only 0.001 cal/g resin (1 cal=4.184 J).

From Eq. (22), the isosteric heat of adsorption can be shown to be:

$$q_{1\pi} = \frac{A}{(b + z_1 x_1)^2}$$

$$\text{where } A = \frac{z_r abz_1}{\lambda \cdot 10^{-3}} \qquad (23)$$

Overload elution predictions of the SMA–NISS model were compared for Eqs. (19) and (23). In both cases, the simulations were performed using the parameters and conditions in Tables 3 and 5 and a sample volume of 500 μl. A typical result is shown in Fig. 8. Clearly, even a small difference in the heat of adsorption (of the order of 10^{-3} cal/g resin) gives significantly different elution profiles. It is clear from this result that accurate measurements of heat of adsorption are essential. Consequently, the assumption made previously with respect to the use of the Clausius-Clapeyron equation is not justified.

3.3. Effects of salt heat of adsorption

Another assumption of the NISS model that needs to be critically reviewed concerns salt–salt interactions. It was previously assumed that the change in the isosteric heat of adsorption for the modulator ion is negligible. This is equivalent to assuming that interactions between these ions on the surface are small compared to protein–protein interactions. This also implies that protein–salt interactions on the surface are negligible.

A simulation study was done on BSA adsorption

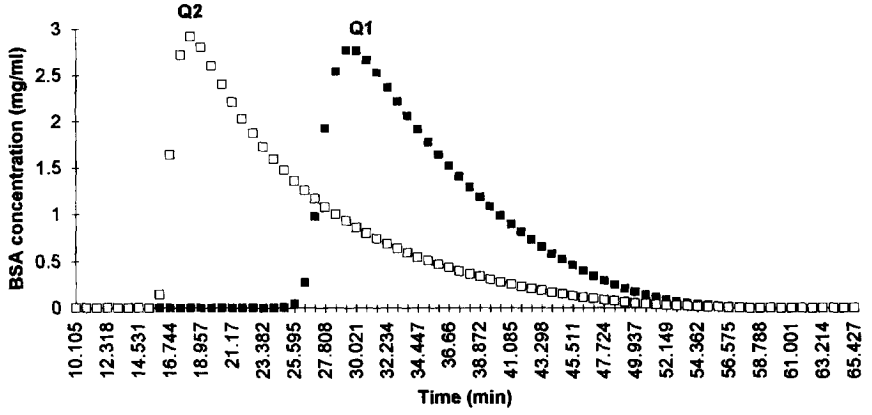

Fig. 8. Effect of heat of adsorption on elution predictions of BSA.

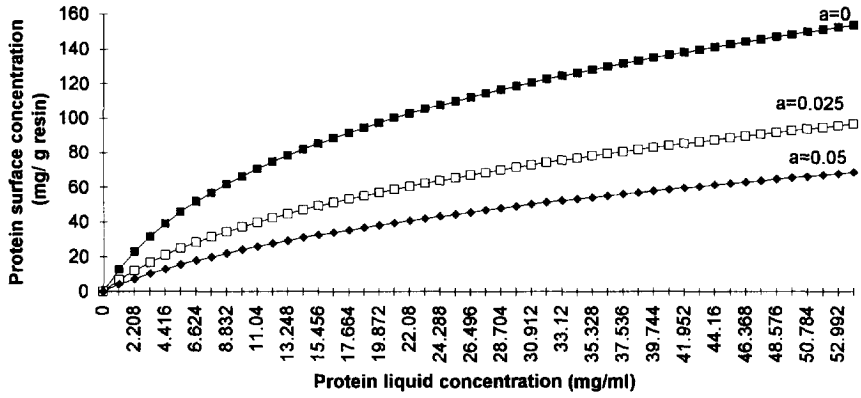

Fig. 9. Effects of salt–salt surface interactions on adsorption.

to analyze its sensitivity to repulsive salt–salt interactions. This analysis used $m=18$ and $\sigma=22$ in the SMA–NISS model and the coefficients in Table 3. It was assumed that

$$q_{n\pi} - q_{n0} = -a \text{ (constant kcal/mol)} \quad (24)$$

In the absence of multicomponent protein data, β_{12} was arbitrarily set to 0.5. Shown in Fig. 9 are adsorption isotherms predicted for three values of a; the value of $a=0$ corresponds to the assumption made originally, and the magnitude selected for the other two predictions (0.025 and 0.05 kcal/mol) correspond to relatively weak salt–salt interactions. Clearly, the predicted protein capacity is very sensitive to the salt–salt lateral interactions and decreases with increasing salt–salt interactions. While this might seem surprising at first, it can be explained by the increase in protein non-ideality (increase in protein surface activity coefficient γ_i^s) due to the increase in 'a' as is shown in Fig. 10. This is a consequence of the model, since the introduction of salt–salt lateral interactions introduces salt–protein interactions (Eq. (8)).

It is hypothesized that an increase in the repulsive interactions between salt molecules reduces the shielding effect salts have on proteins and thus increases the non-ideality in protein behavior. This effect does not significantly increase salt non-ideality

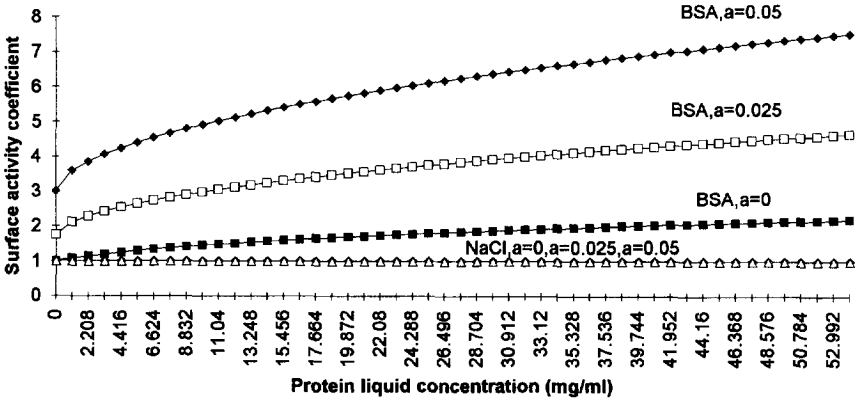

Fig. 10. Effects of salt–salt surface interactions on surface activity coefficients.

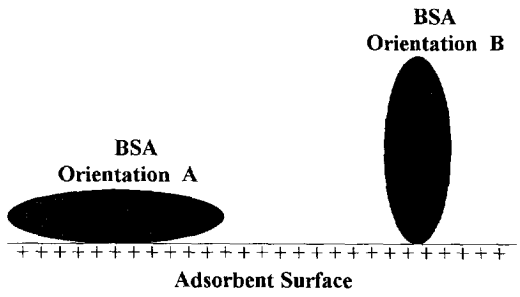

Fig. 11. Selected orientations of adsorbed BSA.

(γ_n^s, Fig. 10), as the protein has a much larger perimeter available for interaction with other proteins and salt molecules.

3.4. Importance of shape factor

All of the above simulations have been performed using the molecular dimensions of the proteins in solution. The protein BSA has been modeled as a prolate ellipsoid of revolution with major axis 140 Å and minor axis 40 Å [21]. When a protein adsorbs on a surface, many orientations are possible. The two orientations of BSA in Fig. 11 were chosen to study the importance of shape factor on adsorption predictions of BSA. Orientations A and B give shape factors of 13.55 and 6.024. The predicted adsorption isotherm at each of these orientations is shown in Fig. 12. As can be seen, the influence of the shape factor is dependent on the magnitude of the salt–salt interactions ('a' value). In the absence of these interactions, the model is insensitive to S_i. However, at higher values of 'a' the isotherm is highly sensitive to this parameter. Also, it should be noted that by reducing the perimeter of interaction (Orientation B) the sensitivity of the adsorption isotherm to 'a' decreases (Fig. 12), which is as expected. The results in Fig. 12 imply that if calorimetric measurements indicate that salt–salt lateral interactions are significant, it is necessary to obtain the shape and orientation of the absorbed form of the protein accurately and to determine if these are a function of surface concentration.

4. Conclusions

This analysis of protein ion-exchange equilibria has led to several significant conclusions. First, it has been shown that in order to correctly characterize steric hindrance and surface interactions between adsorbed molecules with the SMA–NISS model, it is necessary to have an adsorption isotherm as well as ion-exchange heat data. Secondly, since the model is very sensitive to the heat data, accurate calorimetric measurements must be made of the variation of heat of ion exchange with composition. Thirdly, it has been shown that salt–salt interactions on the surface cannot, in general, be neglected relative to protein–protein interactions. Although the surface activity of

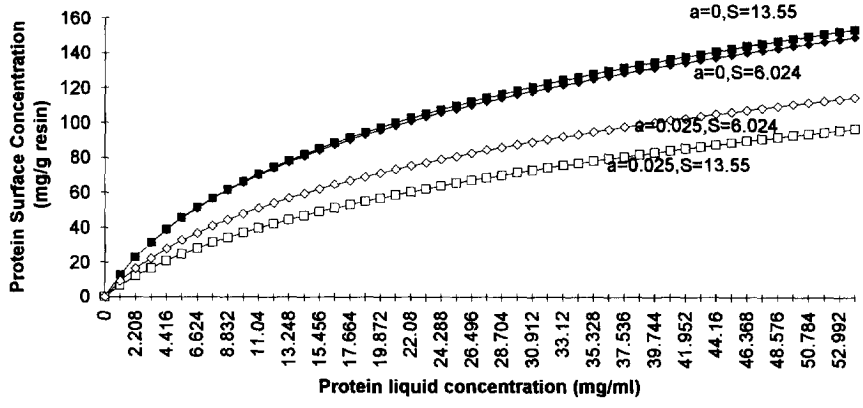

Fig. 12. Effects of shape factor on adsorption behavior.

the salt is relatively constant, the protein surface activity is strongly affected by the salt. It is postulated that repulsive interactions between salts affect the degree of shielding between adsorbed proteins and hence the amount of protein adsorbed. Finally, when salt–salt interactions are significant, it is important to know the shape and orientation of the molecule on the surface, since the adsorption behavior is very sensitive to the perimeter of the molecule available for lateral interactions.

5. Symbols

a	constant (kcal/mol)
a_i	bulk activity of i
a_i^s	surface activity of i
B	Bromley's constant
c_i	bulk concentration (mM)
C	coordination number for adsorbed segments
D_i	effective axial diffusion coefficient (cm^2/min)
e_{ij}	energy of interaction parameter
I	ionic strength (molal)
k	Boltzmann constant
k_i	effective mass transfer coefficient (min^{-1})
k'	elution capacity factor
K_{ni}	equilibrium constant for ion exchange of n,i
L	length of column
m	slope coefficient (Eq. (16))
n	number of components
n_i	surface concentration (mmol/kg resin)
$\overline{n_n}$	surface concentration of available salt ions
$\hat{n}_n$	surface concentration of hindered salt ions
n_i^*	equilibrium surface concentration
N	Avogadro number
Pe_i	Peclet number $=u_0L/D_i$
$q_{n\pi}$	isosteric heat of adsorption at spreading pressure of mixture (kcal/mol)
q_{i0}	isosteric heat of adsorption at zero spreading pressure
Q	heat of adsorption (kcal/kg resin)
S	shape factor
St_i	Stanton number $=k_iL/u_0$
t_0	dead time (min)
T	temperature
u_0	fluid velocity (cm/min) $=L/t_0$
x_i	surface mole fraction of i
$\overline{x_n}$	surface mole fraction of available salt ions
X	dimensionless distance
z_i	charge number of i
z_r	charge number of resin
z_+, z_-	charge on salt cation, anion

5.1. Greek Symbols

α_{ij}	Boltzmann weighting factor
β_{ij}	empirical factor accounts for differences in size and adsorptive properties
ϕ	phase ratio (kg/l)
γ_i^s	surface activity coefficient of i
λ	equivalent ion-exchange capacity of resin (mequiv./kg resin)
σ_i	steric factor
τ	dimensionless time
ω_i	surface fraction

5.2. Subscripts

F	feed
i	protein
n	modulator

5.3. Superscript

s	surface phase

References

[1] F.E. Regnier, Science, 222 (1983) 245.
[2] P.K. de Bokx, P.C. Baarslag and H.P. Urbach, J. Chromatogr., 594 (1992) 9.
[3] P. Jandera and G. Guiochon, J. Chromatogr., 605 (1992) 1.
[4] C. Kemball, E.K. Rideal and E.A. Guggenheim, Trans. Farad. Soc., 44 (1948) 948.
[5] D.M. Ruthven, Principles of Adsorption and Adsorption Processes, Wiley, New York, 1984.
[6] W. Kopachiewicz, M.A. Rounds, J. Fausnaugh and F.E. Regnier, J. Chromatogr., 266 (1983) 3.
[7] M.A. Rounds and F.E. Regnier, J. Chromatogr., 283 (1984) 37.
[8] F.E. Regnier and I. Mazsaroff, Biotech. Prog., 3 (1987) 22.

[9] A. Velayudhan and Cs. Horváth, J. Chromatogr., 443 (1988) 13.
[10] C.A. Brooks and S.M. Cramer, AIChE J., 38 (1992) 1969.
[11] Y. Li and N.G. Pinto, J. Chromatogr. A, 658 (1994) 445.
[12] R.R. Drager and F.E. Regnier, J. Chromatogr., 359 (1986) 147.
[13] D. Kahaner, C. Moler and S. Nash, Numerical Methods and Software, Prentice Hall, Englewood Cliffs, NJ, 1989.
[14] O. Talu and I. Zweibel, AIChE J., 32 (1986) 1263.
[15] G.M. Wilson, J. Am. Chem. Soc., 86 (1964) 127.
[16] L.A. Bromley, AIChE J., 19 (1973) 313.
[17] Y. Li and N.G. Pinto, J. Chromatogr. A, 702 (1995) 113.
[18] O. Talu, Ph.D. Dissertation, Arizona State University, Tempe, AZ, 1984.
[19] R.P. Smith and E.T. Woodburn, AIChE J., 24 (1978) 577.
[20] M.T.W. Hearn, A.N. Hodder and M.I. Aguilar, J. Chromatogr., 443 (1988) 97.
[21] P.G. Squire, P. Moser and C.T. O'Konski, Biochemistry, 7 (1968) 4261.
[22] L. Stryer, Biochemistry, W.H. Freeman, New York, 3rd ed. c1988, 220, 407.